Advances in Reliability, Safety and Security, Part 3 – Kołowrocki, Dąbrowska (eds.)
 ISBN 978-83-68136-15-9 (printed), ISBN 978-83-68136-02-9 (electronic)

Advances in Reliability, Safety and Security

ESREL 2024
Monograph Book Series

Degradation Modelling Of Light Emitting Diodes Using Gaussian Regression Method

Quoc Tiep La, Zdenek Vintr, David Valis

Faculty of Military Technology, University of Defense, Brno, Czech Republic

Abstract

Light-emitting diodes (LEDs) constitute pivotal components applied across diverse domains encompassing lighting, signaling, medicine, and other sectors. Since functioning as luminescent devices, LEDs exhibit a self-heating phenomenon during operation, emanating from internal heat generation. This self-heating phenomenon significantly influences the operational reliability of LEDs, particularly in confined environments, manifested externally by an increase in the temperature of the surrounding environment, which causes the LED's degradation rate to occur faster than expected. Consequently, these impacts of phenomenon must be considered when conducting Accelerated Tests (ATs) for LEDs. This paper introduces a voltage degradation model for LEDs, using the Gaussian regression method. This model is formulated based on voltage data derived from accelerated testing, considering the increased test temperature due to the self-heating effect as an input variable.

Keywords: light-emitting diode, accelerated test, self-heating, Gaussian regression

1. Introduction

Self-heating is a phenomenon inherent to devices, excluding those designed specifically for heat generation, wherein the device is regarded as a heat source due to the presence of a distinct internal resistance. Despite advancements in science and technology, no viable solutions have been proposed to eliminate this internal resistance, necessitating its acknowledgement. This phenomenon substantially influences the performance and operational efficiency of electronic systems and devices, including Electronic Control Units (ECUs) and semiconductor components, etc.

While light-emitting diodes (LEDs) are known for their extended lifespan of up to 50,000 hours in open environments (IESNA, 2008) rendering the impact of self-heating seemingly inconsequential, its significance becomes pronounced in accelerated tests. In scenarios where temperature functions as an acceleration factor, due consideration must be given to this phenomenon. Notably, a mere increase of 10 ^{o}C in temperature leads to a twofold escalation of the degradation of respective devices, underscoring the imperative nature of addressing self-heating in such accelerated testing environments. In ATs, this phenomenon increases the temperature of the surrounding environment and makes the test temperature unstable, which causes the LED's degradation rate to occur faster than expected.

Our survey focused on articles using the keywords "LED," "degradation," "reliability," and "self-heating," revealing limited relevance to these themes. Notably, the work by (Truong et al., 2022) specifically considers the impact of self-heating on Cree EZ1000 LEDs. The methodology involves Accelerated Degradation Tests (ADTs) to capture lumen data at various temperatures. Instead of directly assessing the actual temperature impact during testing, the authors employ mathematical methods to describe and model the self-heating effects.

In contrast, other surveyed articles also employ ADTs for different LED types, incorporating temperature as an acceleration factor at various values. (Pugalenthi et al., 2022) introduce ADTs for both Light Output LEDs and Color LEDs, conducting tests at distinct temperatures and current combinations to evaluate lumen degradation. Similarly, (Enayati et al., 2021) conduct ADTs for Edison Opto Corporation's 3W LED under mild

and severe conditions, recording luminous flux data over extended durations. Notably, temperature data during the test process is regrettably omitted in their investigations.

While the survey reveals a scarcity of relevant articles, the identified works provide valuable insights into the assessment of LED reliability, particularly in the context of self-heating considerations. Further research in this domain could benefit from a more comprehensive exploration of the interplay between temperature, self-heating, and degradation in diverse LED models and conditions.

Obviously, obtaining degradation data, can be called the experimental method is respected in reliability research. In some cases, the data can be used to assess the deterioration process of objects, but in other cases, it is not sufficient for the assessment. Therefore, the modelling approach was proposed and developed as an independent solution or a support, supplement and development solution for the experiment methods. (Tsai et al., 2022) present a physics-based model to study the efficiency droop under high current densities of h-LEDs and c-LEDs using Open-Boundary Quantum LED Software. (Kyatam et al., 2021) propose a method using ANSYS software to assess the reliability of Cree white XLamp XB-D LEDs with impact of Die Carrier. In another way, (Pugalenthi et al., 2022) present a deep learning method based on obtained data using neural networks and Bayesian optimization to predict the lumen degradation of LEDs. (Lim et al., 2022) develop the Gaussian regression with multi-output to validate the reliability of OSRAM golden dragon LEDs with anomaly detection. (Anh et al., 2022) combine statistical techniques and Wiener process to predict mean time to failure and remaining useful life of LEDs based on obtained degradation data and figure out the critical level. (Ibrahim et al., 2021) present a Bayesian networks method to estimate the lifetime of LEDs based on the degradation data of LED components which impact on the lifetime and performance of LEDs. (Valis et al., 2023) develop a model which is backed up by stochastic diffusion process to estimate, determine and predict key reliability measures of LEDs. According to the survey, the data-driven model predominates and is used commonly in LED reliability studies.

The primary objective of this article is to present a systematic experimental methodology designed to monitor meticulously and document the voltage and temperature fluctuations throughout a long-term accelerated testing period, employing a chosen high sample frequency for Light-Emitting Diodes (LEDs). In our modelling approach, we adopt a Bayesian-optimized Multi-Input and Single-Output (MISO) Gaussian process regression framework. This methodology is employed to model the degradation of LEDs effectively, considering temperature variations imposed during the testing phase. The model is established by using voltage degradation data obtained from diverse LEDs, with the additional utilization of other LED data to validate its predictive performance.

2. Proposed methodologies

2.1. Multi-input, single-output Gaussian regression process

Gaussian regression, also known as Gaussian process regression or kriging, is a non-parametric Bayesian approach for regression analysis. It's particularly useful when dealing with problems where the underlying relationships are not known or when the relationships are complex and nonlinear. Suppose that we consider a system with *n*-input variables $\mathbf{X} = (X_1, X_2, \ldots, X_n)$ and single output variable $Y = (y_1, y_2, \ldots, y_m)$. **X,** Y can be rewritten in vector form as $\mathbf{X} = [X_1, X_2, .., X_n]^T$ and $Y = [y_1, y_2, \ldots, y_m]^T$ with m is the number of data points in the training dataset. The aim is to figure out a function $f(\mathbf{X})$ that represents the values of Y in terms of the values of **X**, and can be represent as form:

$$Y = f(\mathbf{X}) + \boldsymbol{\varepsilon} \tag{1}$$

where $\boldsymbol{\varepsilon}$ is a vector of independent and identically distributed Gaussian noise terms. $f(\mathbf{X})$ is vector-valued function representing the latent functions associated with the output. The joint distribution of the latent function in Gaussian Regression is typically modelled as a multivariate normal distribution as given by (Li and Chen, 2016):

$$P(f(\mathbf{X})) \sim GP(\boldsymbol{\mu}, \mathbf{K}) \tag{2}$$

where $GP(\boldsymbol{\mu}, \mathbf{K})$ denotes a multivariate normal distribution; $\boldsymbol{\mu}$ is the mean vector of the latent function and **K** is the covariance matrix of the latent function.

The general form of the covariance function for a multi-input scenario can be expressed as $k(\mathbf{X}, \mathbf{X}')$, in which **X**, **X'** are the input vector associated with different input points. Hence, the matrix **K** is represented by:

$$\mathbf{K} = \left| k(\mathbf{X}_i, \mathbf{X}_j) \right|_{n \times n} \qquad i = 1, .., n;\ j = 1, \ldots, n. \tag{3}$$

Each element of **K** is the covariance function (kernel) that captures the relationships between different input

points. In the context of multi-input and single-output Gaussian regression, the covariance function (kernel) plays a crucial role in modelling the relationships between different input dimensions and capturing the smoothness or correlation in the latent function. Some kernel functions are applied to calculate the value of the elements of **K**, are Radial Basis Function (RBF) Kernel (Gaussian Kernel), Linear Kernel, Polynomial Kernel, Matérn Kernel. The Radial Basis Function (RBF) Kernel and Matérn Kernel are represented as follow:

- Radial Basis Function (RBF) Kernel (Gaussian Kernel) (Kuo et al., 2014):

$$k(\mathbf{X},\mathbf{X}') = \exp\left(-\frac{\|\mathbf{X}-\mathbf{X}'\|^2}{2\ell^2}\right) \tag{4}$$

where ℓ is a length scale parameter that controls the smoothness of the function.

- Matérn Kernel (Tronarp et al., 2018):

$$k(\mathbf{X},\mathbf{X}') = \frac{2^{1-\nu}}{\Gamma(\nu)}\left(\frac{\sqrt{2\nu}\|\mathbf{X}-\mathbf{X}'\|}{\ell}\right)^{\nu} K_{\nu}\left(\frac{\sqrt{2\nu}\|\mathbf{X}-\mathbf{X}'\|}{\ell}\right) \tag{5}$$

in which, ν is a shape parameter and K_ν is the modified Bessel function.

The output variable is considered as a noise-version of $f(\mathbf{X})$ (Li and Chen, 2016):

$$P(Y|f(\mathbf{X})) \sim N(f(\mathbf{X}),\sigma^2) \tag{6}$$

where $N(f(\mathbf{X}),\sigma^2)$ denotes a normal Gaussian distribution and σ^2 is the variance of the observation noise for output variable. The probability density function (PDF) of this normal distribution is given by:

$$P(Y|f(\mathbf{X})) = \frac{1}{\sqrt{2\pi\sigma^2}}\exp\left(-\frac{(Y-f(\mathbf{X}))}{2\sigma^2}\right) \tag{7}$$

In the MISO Gaussian regression, the likelihood function is used in combination with the prior distribution over the latent function (modelled using the covariance function) to obtain the posterior distribution of the latent function given the observed data. The likelihood function models the distribution of the observed output variable Y given the latent function $f(\mathbf{X})$ and the observation noise. Assuming Gaussian noise, the likelihood function is expressed as the probability density function (PDF) of the multivariate normal distribution (Li and Chen, 2016; Maatouk and Bay, 2016):

$$P(Y|\mathbf{X},\boldsymbol{\theta}) = \frac{1}{(2\pi)^{m/2}|\mathbf{K}|^{1/2}}\exp\left(-\frac{1}{2}f(\mathbf{X})-\boldsymbol{\mu}\right)^{T}\mathbf{K}^{-1}(f(\mathbf{X})-\boldsymbol{\mu}) \tag{8}$$

where $(2\pi)^{m/2}|\mathbf{K}|^{1/2}$ is a normalization constant associated with the Gaussian distribution, m is the number of data points in the training dataset, and $\boldsymbol{\theta}$ typically represents the set of hyperparameters associated with the model.

2.2. Learning and optimizing parameter problems

In Gaussian Regression, the challenges of learning and optimization prominently emerge within the domains of model training, hyperparameter tuning, and the prediction of new values to optimize the likelihood of observed data. The optimization of parameters for prediction is centered on fine-tuning hyperparameters to maximize both predictive mean and variance. This is often contextualized within Bayesian optimization, aiming for an efficient exploration of the hyperparameter space. These processes are inherently iterative, involving continuous updates to hyperparameters and subsequent model refitting.

The learning and optimization endeavors revolve around determining an optimal set of parameters associated with the variables **K** and σ^2. Bayesian optimization methods, employ an acquisition function to strategically select the subsequent hyperparameter configuration for evaluation. Commonly utilized acquisition functions encompass Expected Improvement (EI), Probability of Improvement (PI), and Upper Confidence Bound (UCB). The acquisition function plays a crucial role in balancing exploration and exploitation. Its formal expression is articulated as follows (Wu et al., 2019):

$$\boldsymbol{\theta}^* = \arg\max_{\theta}\alpha(\boldsymbol{\theta}|\mathbf{X},Y,GP) \tag{9}$$

in which, $\alpha(\cdot)$ denote the acquisition function and $\boldsymbol{\theta}$ typically represents the set of hyperparameters associated

with the model. Consider the EI as acquisition function we have (Wang and Jin, 2023):

$$EI(\boldsymbol{\theta}) = \mathbb{E}\left[\max\left(f_{\min} - Y_{new}, 0\right)\right] \tag{10}$$

where $f_{\min} = \min(Y)$ denotes the current best. The EI is computed by:

$$EI(\boldsymbol{\theta}) = \sigma_{new}(\boldsymbol{\theta})\left[Z\Phi(Z) + \phi(Z)\right] \tag{11}$$

where $Z = \dfrac{f_{\min} - \mu_{new}}{\sigma_{new}}$ is Z-score value, which measures how many standards deviations σ_{new} the predicted mean μ_{new} of the objective function at the new configuration is away from the current best value; $\Phi(\cdot)$ is the cumulative distribution function (CDF) of the standard normal distribution, and $\phi(\cdot)$ is the probability density function (PDF) of the standard normal distribution. The acquisition function $\boldsymbol{\theta}^*$ is optimized using an Optimization algorithm. This article elucidates the Limited-memory Broyden-Fletcher-Goldfarb-Shanno (L-BFGS) algorithm, a notable optimization technique renowned for its distinctive feature of employing a limited-memory approximation to the Hessian matrix. Unlike conventional methods that involve the direct computation or storage of the entire Hessian matrix, L-BFGS employs a judicious strategy wherein it maintains a low-rank approximation. This approximation is derived from pertinent information gleaned from the most recent iterations, contributing to computational efficiency and reduced memory requirements. The Likelihood function is adopted as the objective function in our analysis. The L-BFGS update at iteration *k* is calculated as follows (Al-Baali, 2001):

$$\boldsymbol{\Delta}_k = \nabla P\left(Y \middle| f(\mathbf{X}_{k+1})\right) - \nabla P\left(Y \middle| f(\mathbf{X}_k)\right) \tag{12}$$

$$\mathbf{S}_k = \mathbf{X}_{k+1} - \mathbf{X}_k \tag{13}$$

$$\boldsymbol{\rho}_k = \frac{1}{\boldsymbol{\Delta}_k^T \mathbf{S}_k} \tag{14}$$

$$\mathbf{H}_{k+1} = \left(\mathbf{I} - \boldsymbol{\rho}_k \mathbf{S}_k \boldsymbol{\Delta}_k^T\right)\mathbf{H}_k\left(I - \boldsymbol{\rho}_k \boldsymbol{\Delta}_k \mathbf{S}_k^T\right) + \boldsymbol{\rho}_k \mathbf{S}_k \mathbf{S}_k^T \tag{15}$$

in which, $\nabla P\left(Y \middle| f(\mathbf{X}_k)\right)$ is the gradient of the objective function at iteration *k*; $\mathbf{X}_k$ is the parameter vector at iteration *k*; $\boldsymbol{\Delta}_k$ is the difference between gradients at iterations *k*+1 and *k*; $\mathbf{S}_k$ is the difference between parameter vectors at iterations *k*+1 and *k*; $\boldsymbol{\rho}_k$ is a scalar used to update the approximation of the inverse Hessian matrix. $\mathbf{H}_k$ is the approximation to the inverse Hessian matrix at iteration *k* and **I** is the identity matrix.

3. Data acquisition and pre-processing

In this section, we describe an Accelerated Test in the laboratory to obtain the degradation data of warm, white LED GT-P10WW339910700 10W. Its specifications is given in Table 1.

Table 1. The parameter of LED GT-P10WW339910700 10W (GETIAN, 2013).

Parameter	Value	Unit
Luminous flux	700 ÷ 800	lm
Forward Voltage	9 ÷11	V
Maximum Forward Current	1050	mA
Thermal Resistance	12	^{o}C/W

In our experimentation, we conducted conventional Accelerated Degradation Tests (ADTs) incorporating a step-stress methodology, wherein temperature served as the primary acceleration factor while the current remained constant at 1050mA. The temperature in the test was incrementally adjusted in a stepwise fashion over time. Data recording occurred every 10 minutes for both voltage degradation and the temperature within the thermal chamber. The observed temperature data reveals that the actual temperature in the thermal chamber consistently exceeds the proposed temperature by approximately 10^{o} C, as shown in Figure 1 (left). In our ADTs, the degradation parameter is voltage, and temperature within the thermal chamber is also measured. This approach is different from previous methodologies. To account for this temperature variation, we recalibrated the test duration to align with an equivalent normal operating temperature (absent thermal stress).This adjustment involved extending the test time in each temperature period, applying an acceleration coefficient calculated according to the Arrhenius equation (IEC 62506, 2013):

$$A_{FT} = e^{\frac{E_a}{k_B}\left(\frac{1}{T_{use}+273}-\frac{1}{T_{test}+273}\right)} \quad (16)$$

where E_a = 0.7 eV is activation energy, k_B = 8.617385·10^{-5} eV/K is Boltzman's constant, T_{use}=35 ^oC is temperature in use and T_{test} [^oC] is temperature in experiment. Using the Arrhenius equation, our calculations indicate that the adjusted time to normal temperature based measured temperature during the ADTs is greater than based on designed test temperature about two times, can be seen in Figure 1 (right). This insight is crucial in understanding the differences between the designed test conditions and the actual test conditions.

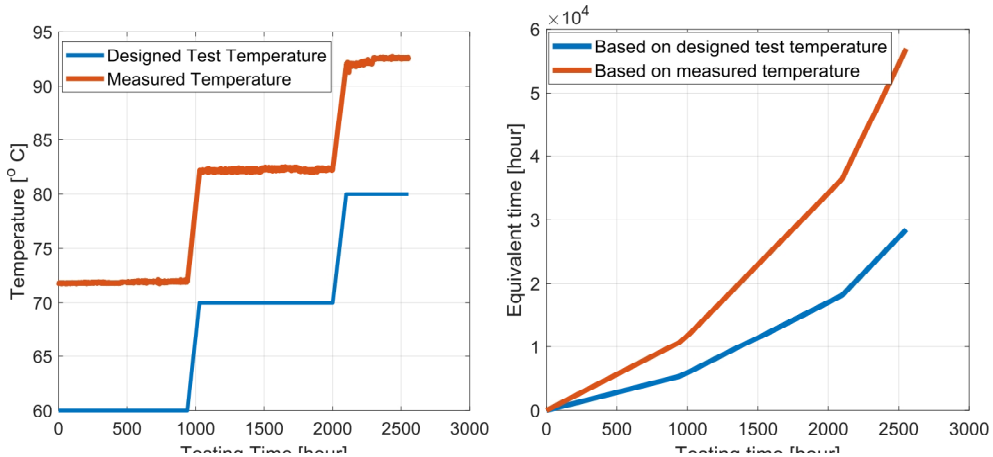

Fig. 1. The graphics plot of the designed test temperature and measured temperature (a); the adjusted equivalent time to normal temperature based on respective temperature (b).

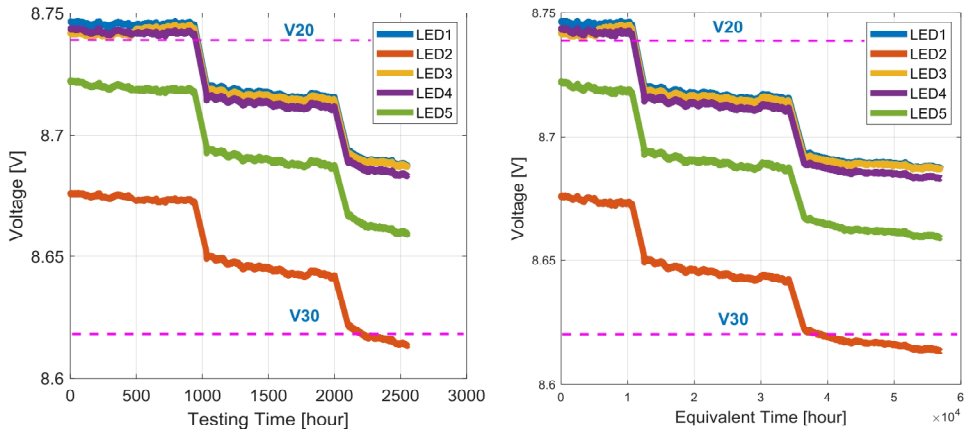

Fig. 2. The graphics plots for obtained voltage degradation data of five LEDs over test time (a); adjusted equivalent time in actual operating temperature based on the measured temperature (b).

The original voltage degradation data of five LEDs is shown in Figure 2. The horizontal line represents critical voltage thresholds for the voltage drop of LEDs corresponding to 20 % (V20) and 30 % (V30) of the initial voltage (Valis et al., 2023). The graph in Figure 2 demonstrates that during the test, at different temperatures, the slopes of the voltage curves are different; in particular, if the temperature increases about 10 ^oC, the gradient of the voltage curve decreases about twice, but if stretching to reach the actual time, they are the relatively same. This data is used to model the voltage degradation process of LEDs in the following sections.

4. Approach Bayesian optimized Gaussian regression method for the voltage degradation of LEDs with self-heating impact

According to the study (Truong et al., 2022), the self-heating phenomenon causes changes inside the LED. However, monitoring and describing these changes are challenges that require respective measurement devices and deep knowledge of LED structure. The self-heating effects are shown through increasing temperature, which makes the temperature in the thermal chamber unstable as the designed testing temperature, mentioned in Section 3. We consider this effect to be a factor making the difference between designed testing conditions and actual testing conditions. Therefore, the aim is to figure out a relationship between voltage degradation, measured temperature, and previous voltage data (at some times in the past).

This section describes the formulation and application of a Bayesian-optimized Gaussian regression to model the voltage degradation of LEDs that incorporates the self-heating phenomenon via the observed temperature within the thermal chamber. We propose a Gaussian regression model, which selects the logarithm of the likelihood function as the main objective function, using the Bayesian Hyperparameter Optimization method in conjunction with the L-BFGS algorithm to train and optimize model parameters. The aim is the maximization of the value of the objective function, with the ultimate goal of discerning optimal functions that accurately encapsulate the intricate relationship between LED voltage degradation, previous voltage data, and obtained temperature data. Each LED's voltage degradation data and corresponding observed temperature data are individually treated as training datasets for our analysis. The model's performance evaluation is conducted through metrics such as Mean Absolute Error (MAE), Root Mean Squared Error (RMSE), R-squared (R^2), and rank correlation (Γ) are given by (Lewis, 1982):

$$RMSE = \sqrt{\frac{1}{n}\sum_{i=1}^{n}(\hat{y}_i - y_i)^2} \tag{17}$$

$$MAE = \frac{1}{n}\sum_{i=1}^{n}\left|\frac{\hat{y}_i - y_i}{y_i}\right| \tag{18}$$

$$R^2 = 1 - \frac{RSS}{TSS} \tag{19}$$

$$\Gamma = \frac{\sum_{i=1}^{n}(\hat{y}_i - \bar{\hat{y}})(y_i - \bar{y})}{\sqrt{\sum_{i=1}^{n}(\hat{y}_i - \bar{\hat{y}})^2 \sum_{i=1}^{n}(y_i - \bar{y})^2}} \tag{20}$$

where: RSS – Residual Sum of squares; TSS – Total Sum of squares; $\hat{y}$ are prediction values, y are observed values of output variables. To validate the robustness and generalizability of the model, it is subjected to validation using data from other LEDs.

5. Results and discussions

Within the confines of this article, the voltage data for LEDs #1 and #2, coupled with the corresponding measured temperature data, is systematically used as the training datasets, called Models #1 and #2. In each figure, the graphics plots are organized from left to right, presenting the results for each case with respective training datasets. This systematic arrangement facilitates a clear and intuitive progression through the visual representations, allowing for easy comparison and interpretation of outcomes across different LED scenarios. The simulation outcomes, encapsulating the model's predictive performance, are graphically presented in Figures 3, 4 and 5, while a comprehensive summary of key metrics and results is provided in Table 2.

Figure 3 illustrates the congruity in the optimization process of The Bayesian Optimization method when employing the voltage data from diverse LEDs as the training dataset after 50 epochs. The process aims to optimize the hyperparameter set of the models consisting of kernel function parameters, sigma, etc., by minimizing the logarithm value of one and the cross-validation loss for regression, measured by five-fold cross-validation. The graph shows that the optimization process results for different LEDs are relatively similar, signifying uniformity during the optimization epochs and the feasibility of using the distinct LEDs' data for training. Figure 4 provides a visual comparison between observed and predicted voltage data across two cases, while Table 2 comprehensively evaluates modelling performance at different stages, namely the Training Stage, Testing Stage, and all data.

In Figure 4, the green dot lines represent observed voltage data acquired from ADTs, and the red solid lines depict predicted voltage data derived from the Gaussian Regression simulation. Based on the simulation results, the two models provide favourable, relatively accurate outcomes, as evidenced by the values of selected performance metrics in Table 2, demonstrating the efficiency of all models. The graphic plots in Figure 4 show that the prediction data is relatively similar to the observed voltage data. When LED#2 data is chosen as the training dataset, respective to Model#2, the models demonstrate better capabilities during the Training Stage, reflected in lower values of RMSE (approximately 36 %). In contrast, Model#1 provides better prediction abilities in the Testing Stage and for all data. Figure 5 indicates the relationships between observed data, predicted data and measured temperature of Models #1 and #2.

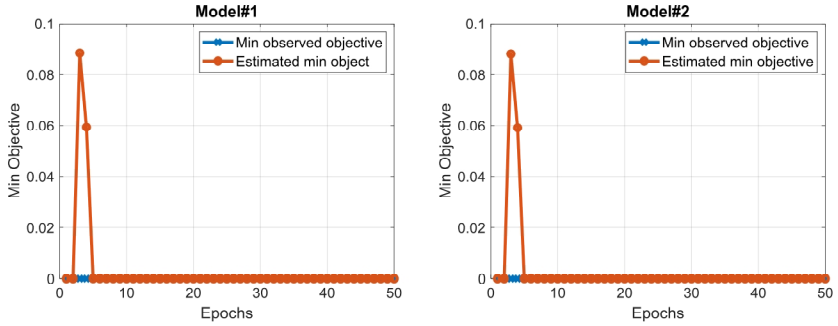

Fig. 3. The results of the optimization process after 50 epochs of Model#1 and #2.

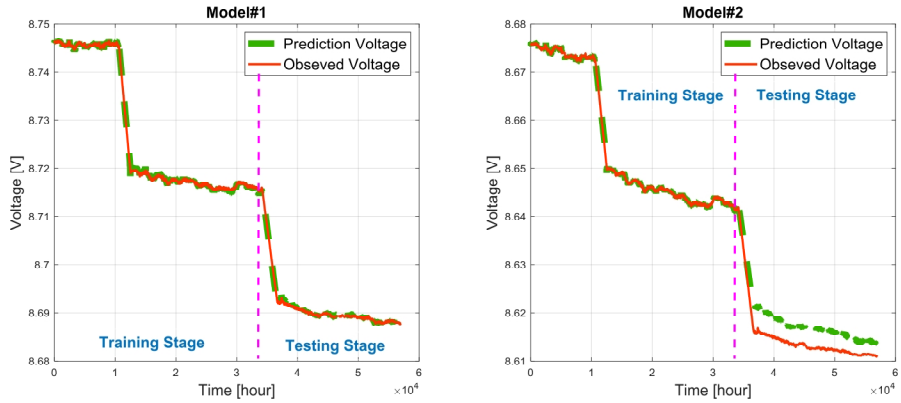

Fig. 4. Comparison results between observed voltage data and prediction voltage data of Model#1 and #2.

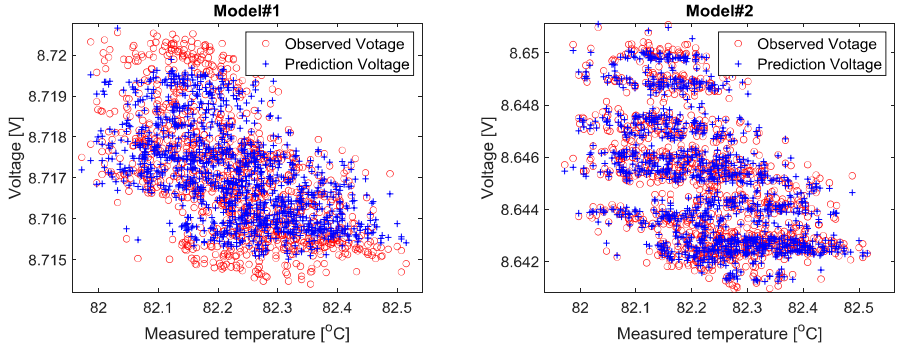

Fig. 5. The relationships between the observed, predicted voltage and measured temperature for Model#1 and #2

Table 2. Performance comparison of two models in the Training Stage, Testing Stage and for all data.

Metrics	Model#1	Model#2
	Training Stage	
LogLikelihood(*)	4.1735e3	1.23e4
MAE	0.00025	0.00016
RMSE	0.00048	0.00021
R-Squared	0.9989	0.9998
Rank-Correlation	0.9868	0.9947
	Testing Stage	
MAE	0.00029	0.00345
RMSE	0.00075	0.00363
R-Squared	0.9867	0.9704
Rank-Correlation	0.9782	0.9925
	All data	
MAE	0.00026	0.00082
RMSE	0.00054	0.00163
R-Squared	0.9993	0.9955
Rank-Correlation	0.9930	0.9972

In order to assess the adaptability of the proposed model, the voltage degradation data from other LEDs are used as validation datasets for each model. The performance metrics mentioned earlier are applicable for verification purposes. The validation results are given in Figures 6 and 7, along with a performance presentation in Table 3. Figure 6 visually illustrates the comparisons observed and predicted voltage data for LED#3, #4, and #5 using Models #1 and #2. Meanwhile, Figure 7 illustrates the boxplot distribution of errors for the corresponding LEDs and the error distribution of the selected training LEDs to capture the spread and central tendencies of errors observed in the model predictions for each model.

Table 3. Validation results of two models with the voltage data of other LEDs.

Metrics		Model#1	Model#2
MAE	LED#3	0.00053	0.0366
	LED#4	0.00094	0.0356
	LED#5	0.0067	0.0243
RMSE	LED#3	0.00078	0.0367
	LED#4	0.0011	0.0357
	LED#5	0.0067	0.0243
R-Squared	LED#3	0.9937	0.9843
	LED#4	0.9943	0.9894
	LED#5	0.9950	0.9911
Rank-Correlation	LED#3	0.9959	0.9961
	LED#4	0.9920	0.9912
	LED#5	0.9960	0.9963

The validation results highlight the robust performance of all models when using training datasets of different LEDs. Based on the simulation results, all models demonstrate good predictability for other LED data, validated by the value of performance metrics in Table 3. However, Model #1 provides better predictability for all LEDs #3, #4, and #5 than Model#2, and the prediction results for these LEDs are higher than the observed data, as shown in Figure 6 (left) and Figure 7 (left) (mean of errors is negative). In contrast, Model#2 provides smaller prediction results than the observed data, as seen in Figure 6 (right) and Figure 7 (right) (mean of errors is positive). The difference between the prediction data and observed data of Model#1 is the highest for LED#5, approximately 0.01 V, while this difference in Model#2 is the highest for LED#3 and #4, approximately 0.03 V. These differences are minor when compared to the voltage values of LEDs, but relatively significant when compared to their voltage variation range. This observation is substantiated by the visual distance between

observed data and predicted data for each LED, highlighting nuanced differences in predictive accuracy across the models.

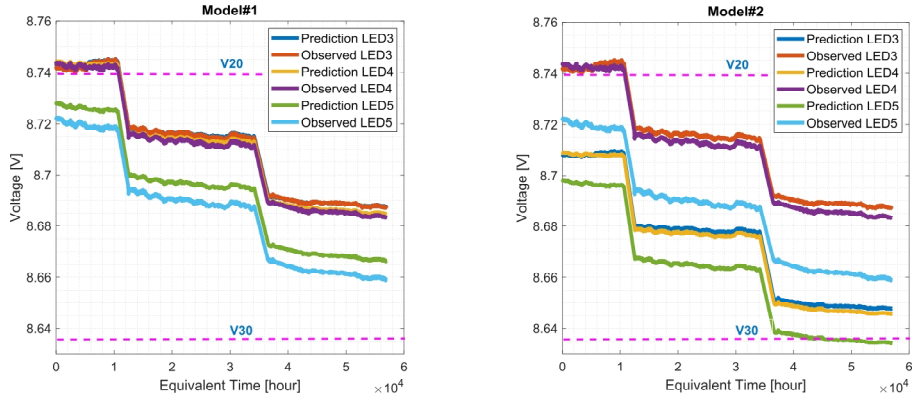

Fig. 6. Comparison of the predictability of all models for the voltage data of other LEDs

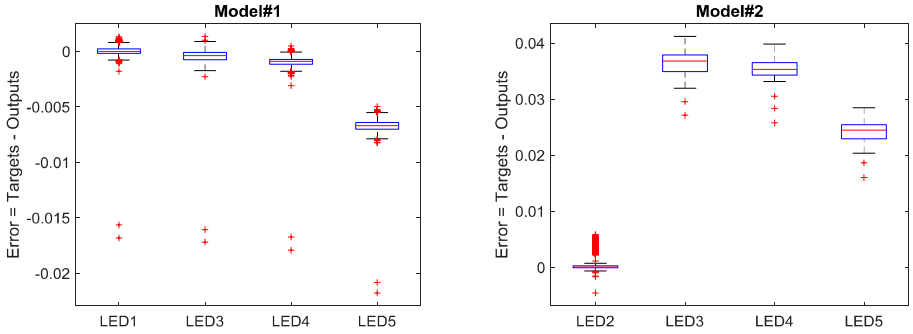

Fig. 7. Boxplot distribution of errors for LEDs in two modelling cases.

In summary, the results collectively indicate that all models provide adaptability, suggesting a comparable training trajectory regardless of the specific LED under consideration, demonstrating generalizability, and showcasing a robust capacity to capture underlying patterns across LED voltage data. These models are effectively applied for modelling the voltage degradation of LEDs in the proposed ADTs. The subtle performance variations among the models underscore the importance of careful consideration and selection based on specific LED datasets and desired predictive outcomes.

6. Conclusions

In this study, a conventional Accelerated Degradation Test is conducted to acquire voltage degradation data, employing stepwise temperature changes and maintaining a constant current. This ADT distinguishes itself from previous studies by focusing on voltage as the monitored degradation parameter and concurrently recording the temperature within the thermal chamber with the high sample frequency. The Bayesian-Optimized Gaussian Regression is then used to model the voltage degradation, utilizing the observed data of each LED and the measured temperature as the training dataset. Various metrics are utilized to assess the model's performance, and validation is conducted across diverse LED datasets.

The findings reveal that all models provide generalizability, demonstrating a robust capacity and strong predictability. This indicates their suitability for effectively modelling the voltage degradation of LEDs based on the acquired data. The study provides valuable insights into the performance and adaptability of the Bayesian-Optimized Gaussian Regression model, underscoring its potential for accurately characterizing the voltage

degradation behaviour of LED in the context of proposed accelerated testing.

In future research endeavours, our focus will extend to conducting varied Accelerated Degradation Tests for LEDs, aiming to obtain diverse degradation data. This comprehensive approach seeks to provide a holistic view of the degradation process of LEDs under different conditions. Additionally, we plan to evaluate the performance of Gaussian Regression across this diverse degradation data to assess the model's efficiency. Simultaneously, our research will involve the simulation of alternative models, enabling a comparative analysis of their effectiveness in handling different datasets of LEDs. This comparative evaluation will contribute to a nuanced understanding of the strengths and limitations of various modelling approaches, ultimately guiding the selection of the most suitable methodology for accurately capturing the intricate degradation patterns of LEDs under varying conditions.

Acknowledgements

The paper has been prepared with the support of the Ministry of Defence of the Czech Republic – Project for the Development of the Organization DZRO VAROPS and Specific Research Project SV22-202.

References

Al-Baali, M. 2001. Extra-Updates Criterion for the Limited Memory BFGS Algorithm for Large Scale Nonlinear Optimization. Journal of Complexity 18, 557-572.

Anh, D. H., Vintr, Z., Valis, D. 2022. An approach in determining the critical level of degradation based on results of accelerated test. Maintenance and Reliability 24, 330 - 337, DOI: 10.17531/ein.2022.2.14.

Enayati, J., Rahimnejad, A., Gadsden, S.A. 2021. LED Reliability Assessment Using a Novel Monte Carlo-Based Algorithm. IEEE Transactions On Device And Materials Reliability 21, 338 - 347.

GETIAN. 2013. Specification For Approval Model GT-P10WW339910700. ShenZen GeTian Optoelectronics Co.,.

Ibrahim, M.S., Fan, J., Yung, W.K.C., Jing, Z., Fan, X., Driel, W.V., Zhang, G. 2021. System level reliability assessment for high power light-emitting diode lamp based on a Bayesian network method. Measurement 176, DOI: 10.1016/j.measurement.2021.109191.

IEC 62506. 2013. Methods for product accelerated testing. IEC.

IESNA. 2008. IES Approved Method: Measuring Lumen Maintenance of LED Light. IES Subcomm. Solid-State Light. IES Test. Proced. Commun., Standard IES, 1-7.

Kuo, B. C., Ho, H.H., Li, C.H., Hung, C.C., Taur, J.S. 2014. A Kernel-Based Feature Selection Method for SVM With RBF Kernel for Hyperspectral Image Classification. IEEE Journal Of Selected Topics in Applied Earth Observations and Remote Sensing 7, 317 - 326.

Kyatam, S., Alves, L.N., Maslovski, S., Mendes, J.C. 2021. Impact of Die Carrier on Reliability of Power LEDs. Journal of The Electron Devices Society 9, DOI: 10.1109/JEDS.2021.3115027.

Lewis, C.D., 1982. Industrial and business forecasting methods : a practical guide to exponential smoothing and curve fitting. London: Butterworth Scientific.

Li, P. and Chen, S., 2016. A review on Gaussian Process Latent Variable Models. CAAI Transactions on Intelligence Technology, 366-376.

Lim, S.L.H., Duong, P.L.T., Park, H., Raghavan, N. 2022. Expedient validation of LED reliability with anomaly detection through multi-output Gaussian process regression. Microelectronics Reliability 138, DOI: 10.1016/j.microrel.2022.114624.

Maatouk, H., Bay, X. 2016. A new rejection sampling method for truncated multivariate Gaussian random variables restricted to convex sets. Springer Proceedings in Mathematics & Statistics, 521-530. Springer.

Pugalenthi, K., Lim, S.L.H., Park, H., Hussain, S., Raghavan, N. 2022. Prognosis of LED lumen degradation using Bayesian optimized neural network approach. Microelectronics Reliability 138, DOI: 10.1016/j.microrel.2022.114728.

Tronarp, F., Karvonen, T., Sarkka, S. 2018. Mixture Representation of The Matérn Class with Applications in State Space Approzimations and Bayesian Quadrature. IEEE 28th International Workshop on Machine Learning for Signal Processing (MLSP). DOI: 10.1109/MLSP.2018.8516992. Aalborg, Denmark: IEEE.

Truong, M.T., Do, P., Mendizabal, L., Iung, B. 2022. An improved accelerated degradation model for LED reliability assessment with self-heating impacts. Microelectronics Reliability 128, DOI: 10.1016/j.microrel.2021.114428.

Tsai, Y.C., Leburton, J.P., Bayram, C. 2022. Quenching of the Efficiency Droop in Cubic Phase InGaAlN Light-Emitting Diodes. IEEE Transactions On Electron Devices 69, 3240-3245, DOI: 10.1109/TED.2022.3167645.

Valis, D., Forbelska, M., Vintr, Z., La, Q.T., Leuchter, J. 2023. Perspective estimation of light emitting diode reliability measures based on multiply accelerated long run stress testing backed up by stochastic diffusion process. Measurement 206, DOI: 10.1016/j.measurement.2022.112222.

Wang, X., Jin, Y., 2023. A New Expected Improvement Acquisition Function for Expensive Multi-Objective Optimization. 2023 5th International Conference on Data-driven Optimization of Complex Systems (DOCS). Tianjin, China: IEEE.

Wu, J., Chen, X.Y., Zhang, H., Xiong, L.D., Lei, H., Deng, S.H. 2019. Hyperparameter Optimization for Machine Learning Models Based on Bayesian Optimization. Journal of Electronic Science and Technology 17, 26-40.